Hindawi
Geofluids
Volume 2022, Article ID 6208096, 10 pages
https://doi.org/10.1155/2022/6208096

Research Article

Experimental Study on Nanomechanical Properties of Yunnan Red-Bed Mudstone

Xian Ye,[1,2] Yongcai Liu,[1,2] Haibin Xue,[1,3] Guo Li,[1,2] and Jin Xing[3]

[1]*National Engineering Laboratory for Surface Transportation Weather Impacts Prevention, Broadvision Engineering Consultants Co. Ltd., Kunming, Yunnan 650041, China*
[2]*Yunnan Communications Investment & Construction Group Co. Ltd., Kunming, Yunnan 650000, China*
[3]*Institute of Rock and Soil Mechanics, Xi'an University of Technology, Xi'an 710048, China*

Correspondence should be addressed to Haibin Xue; xhbyts2013@163.com

Received 19 November 2021; Revised 20 April 2022; Accepted 30 May 2022; Published 7 July 2022

Academic Editor: Peng Hou

As a natural building material and building environment, red-bed mudstone has special engineering properties due to its special formation conditions. The engineering disaster caused by these special properties is becoming increasingly prominent. Therefore, it is of great theoretical significance and practical engineering value to study the macro- and micromechanical properties of red-bed mudstone. Nanoindentation mechanical tests are carried out on the red-bed mudstone from Chuxiong, Jingdong, and Nanhua in Yunnan. The microstructure, residual indentation morphology, and nanomechanical parameters of red-bed mudstone in different areas are compared and analyzed. The results show that the load-displacement curves can be divided into four stages, which are the compaction stage, linear elastic stage, holding stage, and unloading stage. Under the same loading and holding time conditions, sample 3 (Nanhua) has the deepest residual indentation, and SEM tests show that the damage to indentation is obvious. Sample 2 (Jingdong) has the shallowest residual indentation. The indentation morphology is complete and the size is small by SEM tests. The residual indentation depth of sample 1 (Chuxiong) is between sample 2 and sample 3. The average elastic modulus of sample 1 (Chuxiong) is 38.0 ± 2.29 GPa. The average hardness is 1.36 ± 0.42 GPa, and the fracture toughness is 0.966 ± 0.048 MPa·m$^{0.5}$. The average elastic modulus of sample 2 (Jingdong) is 40.1 ± 2.03 GPa. The average hardness is 1.71 ± 0.35 GPa, and the fracture toughness is 1.142 ± 0.053 MPa·m$^{0.5}$. However, the average elastic modulus of sample 3 (Nanhua) is 25.1 ± 2.53 GPa. The average hardness is 0.61 ± 0.21 GPa, and the fracture toughness is 0.507 ± 0.043 MPa·m$^{0.5}$. Overall, the elastic modulus and the hardness of sample 2 (Jingdong) are the greatest because of its high quartz crystal content. It shows that the nanomechanical properties of red-bed mudstone in Jingdong are better than those in Chuxiong and Nanhua. The results can provide a basis for revealing the regional differences in macroscopic mechanical properties of Yunnan red-bed mudstone.

1. Introduction

Yunnan red-bed mudstone is widely used in engineering constructions as natural building material and building environment. Because of the particular formation conditions, it has special engineering properties. With the planning and construction of the Yunnan expressway and railway network, more and more red-bed mudstone engineering disasters are prominent. It is of great significance to understand and master the macro- and micromechanical properties of red-bed mudstone for engineering constructions. At present, the macroscopic mechanical properties of red-bed mudstone are mainly studied by laboratory tests and in situ tests. The microproperty study mainly focuses on the semiquantitative analysis of mineral composition by XRD and the surface morphology by SEM. These studies mainly describe the microphysical properties of red-bed mudstone, but there are relatively few studies on micromechanical indexes.

Nanoindentation is one of the important methods for nondestructive testing of material mechanical properties.

This technology was first proposed by Kalei in 1968 [1], and the range of mechanical tests is at micro- and nanoscale, providing a possibility for the mineral mechanical test. Through the development of Oliver and Pharr [2], the load-displacement curve of the indentation point can be obtained at micro- and nanoscale, and elastic modulus, hardness, fracture toughness, and other parameters can be obtained to provide convenience for the study of material micro- and nanoproperties. At first, the technology is widely used in metal, film, coating, ceramics, glass, and polymer fields. With the development of microscopic rock mechanics, nanoindentation technology has been applied to study rock mechanical properties. Compared with the macromechanical property test of rock, the advantage of the nanoindentation test is that mechanical parameters can be obtained only with a small sample.

The loading rate affects the mechanical behavior of shale in nanoindentation by Shi et al. [3]. The influence of retention time on the hardness, Young's modulus, and creep characteristics of shale was discussed by Shi et al. [4]. Using nanoindentation technology, shale nanomechanical indexes such as elastic modulus, hardness, and fracture toughness were obtained by Liu et al. [5]. Elastoplastic mechanical properties of mudstone clay minerals and detrital minerals in coal rock mass were analyzed, and the influence of quartz and kaolinite on mechanical properties of coal rock mass was discussed by Sun et al. [6, 7]. Elastic modulus of quartz, feldspar, and mica in granite was obtained, and the macromechanical index of granite was obtained by the scaling upgrade method by Zhang et al. [8]. Based on nanoindentation technology, an estimation model of coal fracture strength was proposed, and fracture energy and fracture zone were estimated by using brittle failure theory and inrush phenomenon on the loading curve by Manjunath and Jha [9]. Mechanical properties of coal samples under the conditions of drying and saturated salt solution were studied through nanoindentation tests. The results were compared with those obtained by the acoustic wave test method, and the limitation of the acoustic wave test method was pointed out by Zhang et al. [10]. Hardness and elastic modulus of shale were analyzed and discussed by using indentation technology, and the relationship between the macroscopic and microscopic mechanical properties was evaluated, and a calculation model for rock mechanical parameters at the nanometer scale was proposed by Chen et al. [11]. Through nanoindentation technology, elastic modulus, hardness, fracture toughness, and other mechanical parameters of bedded shale of Lower Silurian Longmaxi Formation of Youyang area in southeast Chongqing were obtained by Shi et al. [12]. Through nanoindentation technology, the influence of water-rock interaction on shear mechanical properties of granite fractures was studied, and it was found that granite fractures were more likely to be damaged after long-term immersing by Dou et al. [13]. The microscopic mechanical properties of shale taken from Longmaxi Formation in the southern Sichuan area were studied by introducing nanoindentation technology by Liu et al. [14]. A set of nano- and micromechanical data for shale samples was provided to constrain the macroscopic mechanical properties determined by the shale microstructure by Graham et al. [15]. The influence of organic matter on shale mechanical properties was studied by Zhao et al. [16]. At present, there are few studies on the nanomechanical properties of red mudstone.

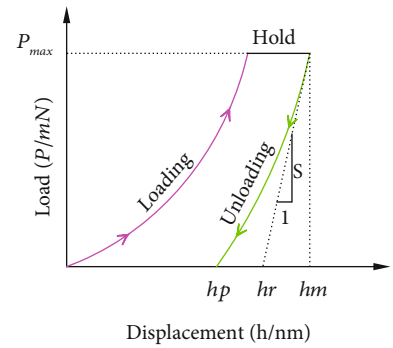

Figure 1: Typical load-displacement curve of single nanoindentation.

Yunnan red mudstone has the characteristics of low strength, weak permeability, and strong hydrophilicity, and it is easy to disintegrate, weather, and be softened after absorbing water. However, the success rate of macrotest sampling is very low and very difficult. Hence, it is very difficult to prepare samples and control test conditions for laboratory macrotests. The above problems can be avoided to a certain extent by nanoindentation technology from the microscopic point of view. In this paper, nanoindentation technology is used to carry out experimental research on red-bed mudstone from three different areas in Yunnan province. Nanomechanical property indexes of samples from different areas are obtained. Residual indentation morphology of samples from different areas is observed by SEM. Combined with a thin section examination of rock, the relationship between nanomechanical properties and mineral composition of red-bed mudstone in different areas of Yunnan is analyzed. The results provide a theoretical basis for revealing the regional differences in macroscopic mechanical properties of Yunnan red-bed mudstone.

2. Basic Principles and Test Procedures of Nanoindentation Technology

2.1. Basic Principles of Nanoindentation. The nanoindentation test is a microscopic measurement technique for continuous control and measurement of load and displacement. The mechanical properties such as elastic modulus, hardness, and fracture toughness are measured at the nanoscale by contact mechanics analysis. In the nanoindentation test, the indenter is pressed into the sample gradually, the elastic deformation of the sample near the indenter first occurs, and the plastic deformation of the sample begins to produce with the increase of load. Finally, an indentation matching the indenter shape appears in the sample. The load-displacement curves can be obtained by nanoindentation tests. Mechanical indexes such as elastic modulus and hardness of rock at the microscopic scale can be calculated by the

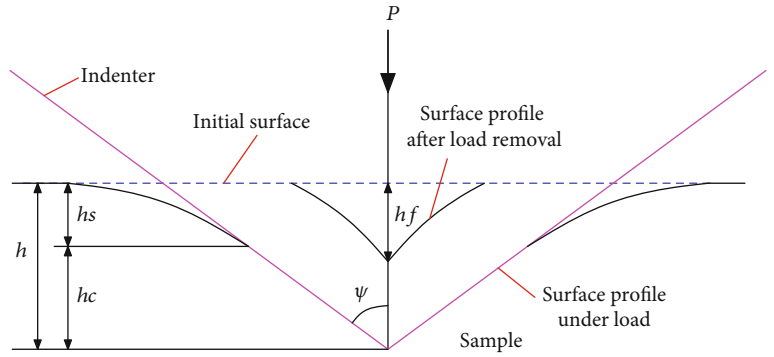

Figure 2: Schematic diagram of loading and unloading process [17].

load-displacement curve, as shown in Figure 1. The specific calculation method is as follows:

$$S = \frac{dP}{dh}|_{h=h_m},$$
$$H = \frac{P_{\max}}{A_c},$$
$$E_r = \frac{\sqrt{\pi}}{2\beta} \cdot \frac{S}{\sqrt{A}}, \quad (1)$$
$$\frac{1}{E_r} = \frac{(1-\nu^2)}{E} + \frac{(1-\nu_i^2)}{E_i},$$

where P is load (mN), h is indenter displacement (nm), h_m is maximum indenter displacement (nm), S is material stiffness (N/m), H is material hardness (GPa), A is contact area (nm^2), ν is material Poisson's ratio, E_r is reduced modulus (GPa), E is material elastic modulus (GPa), β is a constant related to indenter geometry, E_i is indenter elastic modulus (GPa) and is 1141 GPa, and ν_i is indenter Poisson's ratio and is 0.07.

For the *Berkovich* indenter, the relationship between indenter contact depth and projected area of the contact area is as follows:

$$A_c = 3\sqrt{3}\tan^2\theta \cdot h_c^2, \quad (2)$$

where θ is the angle between the indenter central axis and the indenter side and is 65.27°. Therefore, $A_c = 24.56h_c^2$. h_c is contact depth, as shown in Figure 2. The specific expression is as follows:

$$h_c = h - \varepsilon\frac{P}{S}, \quad (3)$$

where ε is constant related to indenter shape. For the Berkovich indenter, $\varepsilon = 0.75$.

2.2. Fracture Toughness Calculation. Fracture toughness (K_c) is the material inherent property and represents the ability to resist crack propagation under external load [18]. It can be calculated with the energy analysis method by using the nanoindentation test. Although the indentation test is a non-destructive test and is used to evaluate elastic properties of materials in most cases, the stress intensity factor at the crack tip reaches the critical value with the increase of load

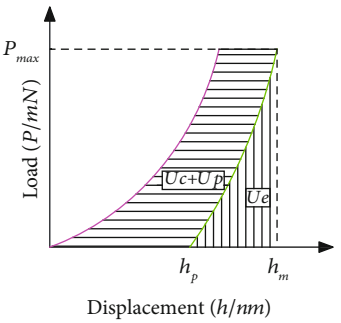

Figure 3: Schematic diagram of total energy and unloading energy.

Figure 4: Agilent nanoindenter G200.

(a) Chuxiong (b) Jingdong (c) Nanhua

Figure 5: Diagram of representative mudstone samples.

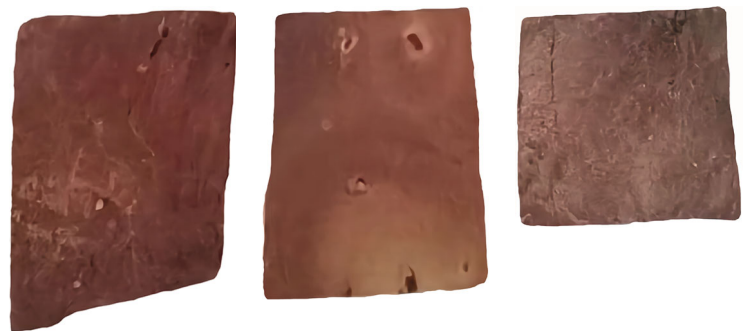

(a) Sample 1 (Chuxiong) (b) Sample 2 (Jingdong) (c) Sample 3 (Nanhua)

Figure 6: Nanoindentation sample.

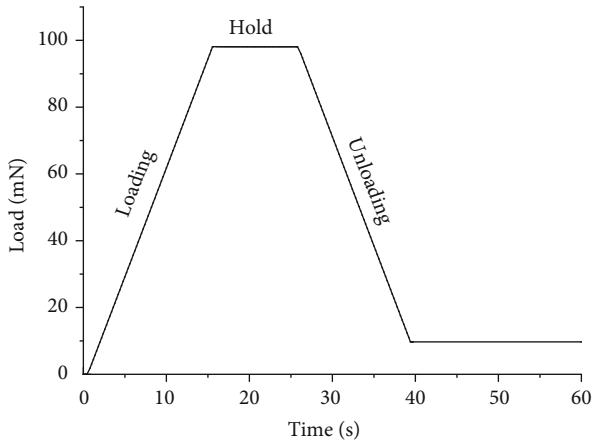

Figure 7: Load-time curve of nanoindentation.

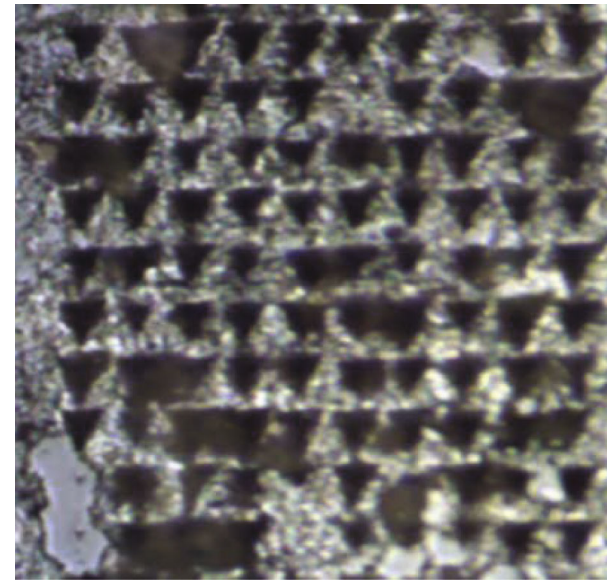

Figure 8: Indentation bitmap.

[19]. In other words, there are two situations in the indentation process. One is that there is no microcrack and the whole indentation process is an elastic-plastic deformation process; the other is that cracks continue to initiate and propagate as the load increases.

The principle of determining rock fracture toughness with the energy analysis method is as follows.

According to Cheng's theory [18], the total input energy (U_t) is the sum of fracture energy (U_c), plastic energy (U_p), and elastic energy (U_e), as shown in Figure 3. Fracture energy can be expressed as follows:

$$U_t = U_c + U_e + U_p, \tag{4}$$

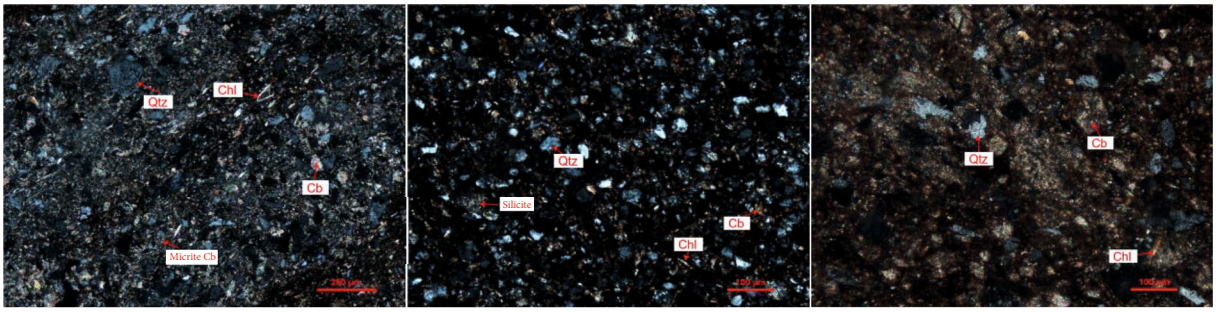

Figure 9: Thin-section mesostructure of Yunnan red-bed mudstone in three regions.

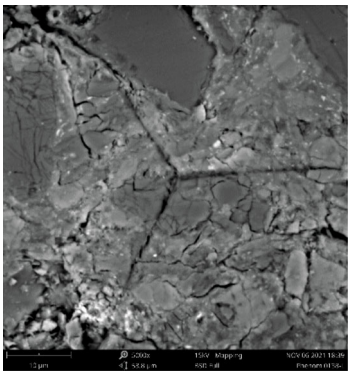

(a) Sample 1 (Chuxiong)

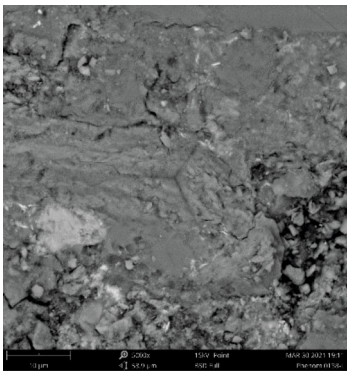

(b) Sample 2 (Jingdong)

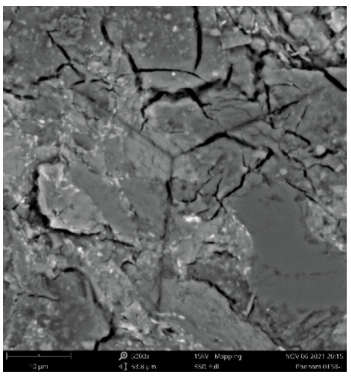

(c) Sample 3 (Nanhua)

Figure 10: Comparative analysis of residual indentation morphology of Yunnan red-bed mudstone in the three regions.

where the relationship between total energy (U_t) and plastic energy (U_p) is as follows:

$$\frac{U_p}{U_t} = 1 - \left[\frac{1 - 3\left(h_p/h_m\right)^2 + 2\left(h_p/h_m\right)^3}{1 - \left(h_p/h_m\right)^2}\right]. \tag{5}$$

The calculation formula of total energy (U_t) is as follows:

$$U_t = \int_0^{h_m} P dh. \tag{6}$$

According to linear elastic fracture mechanics, the critical energy release rate (G_c) is the energy released per unit area during the crack propagation process and can be calculated as follows:

$$G_c = \frac{\partial U_c}{\partial A_c} = \frac{U_c}{A_{max}}, \tag{7}$$

where for *Berkovich* indenter, $A_{max} = 24.56{h_m}^2$.

Therefore, the fracture toughness can be expressed as follows:

$$K_c = \sqrt{G_c \times E_r} \approx \sqrt{\frac{G_c \times E}{1 - \nu^2}}. \tag{8}$$

2.3. Nanoindentation Experimental Equipment. The nanoindentation tests are carried out on the Agilent nanoindenter

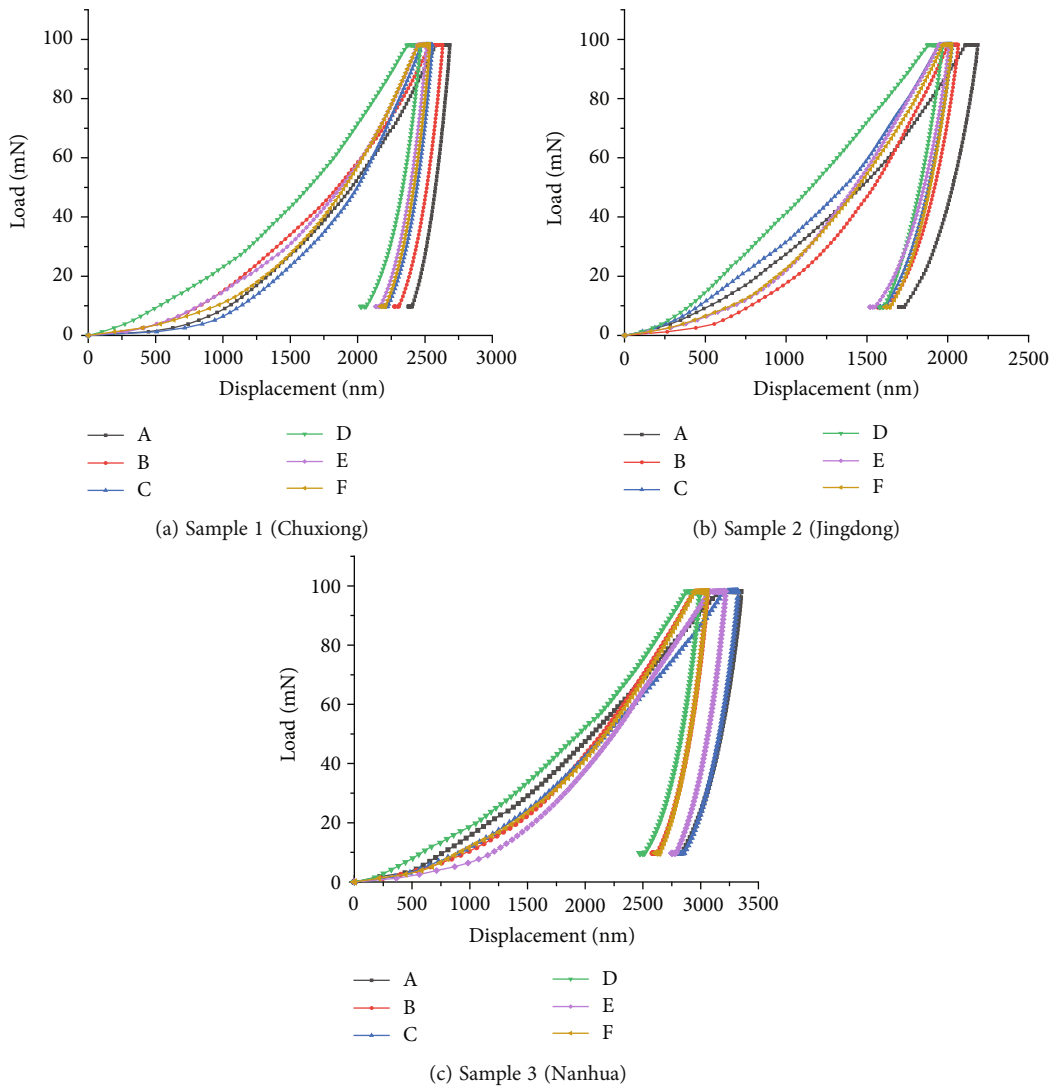

Figure 11: Nanoindentation load-displacement curves of Yunnan red-bed mudstone samples in three regions.

G200, as shown in Figure 4. The maximum load is 500 mN, and the load resolution is 50 nN. The Berkovich indenter is selected for this test. The maximum indenter displacement is 1.5 mm. The maximum indentation depth is 500 μm, and the displacement resolution is 0.01 nm.

2.4. Experimental Procedure. Representative mudstone samples from three regions of Chuxiong, Jingdong, and Nanhua in Yunnan are successively named sample 1, sample 2, and sample 3, as shown in Figure 5.

The indentation area is set as the dot matrix. The dot matrix of Chuxiong (sample 1), Jingdong (sample 2), and Nanhua (sample 3) is 10×10, 8×8, and 10×10, respectively. The horizontal and vertical distance of the indentation points is 50 μm. The specific experimental procedure is as follows.

2.4.1. Cutting the Sample. A large red-bed mudstone sample was precisely cut. The irregular red-bed mudstone blocks were cut into thin slices with a thickness of about 5 mm and cross-section of about 10 mm × 10 mm.

2.4.2. Polishing the Sample. The samples were polished by using 600-, 800-, 1000-, 2000-, 3000-, 5000-, and 7000-grit paper in sequence. The polishing time for 7000-grit paper was no less than 0.5 hours to ensure that the sample surface was flat and smooth.

2.4.3. Cleaning the Sample. The sample was cleaned ultrasonically with anhydrous ethanol to make the sample surface have no impurities.

2.4.4. Drying the Sample. Finally, the samples were placed in an oven at 50°C for no less than 24 hours to ensure that the sample was completely dry. After that, the sample was stored in an airtight container for later use. The prepared sample of red-bed mudstone is shown in Figure 6.

2.4.5. Observing the Sample Surface Microstructure. The sample surface microstructure was observed to find a

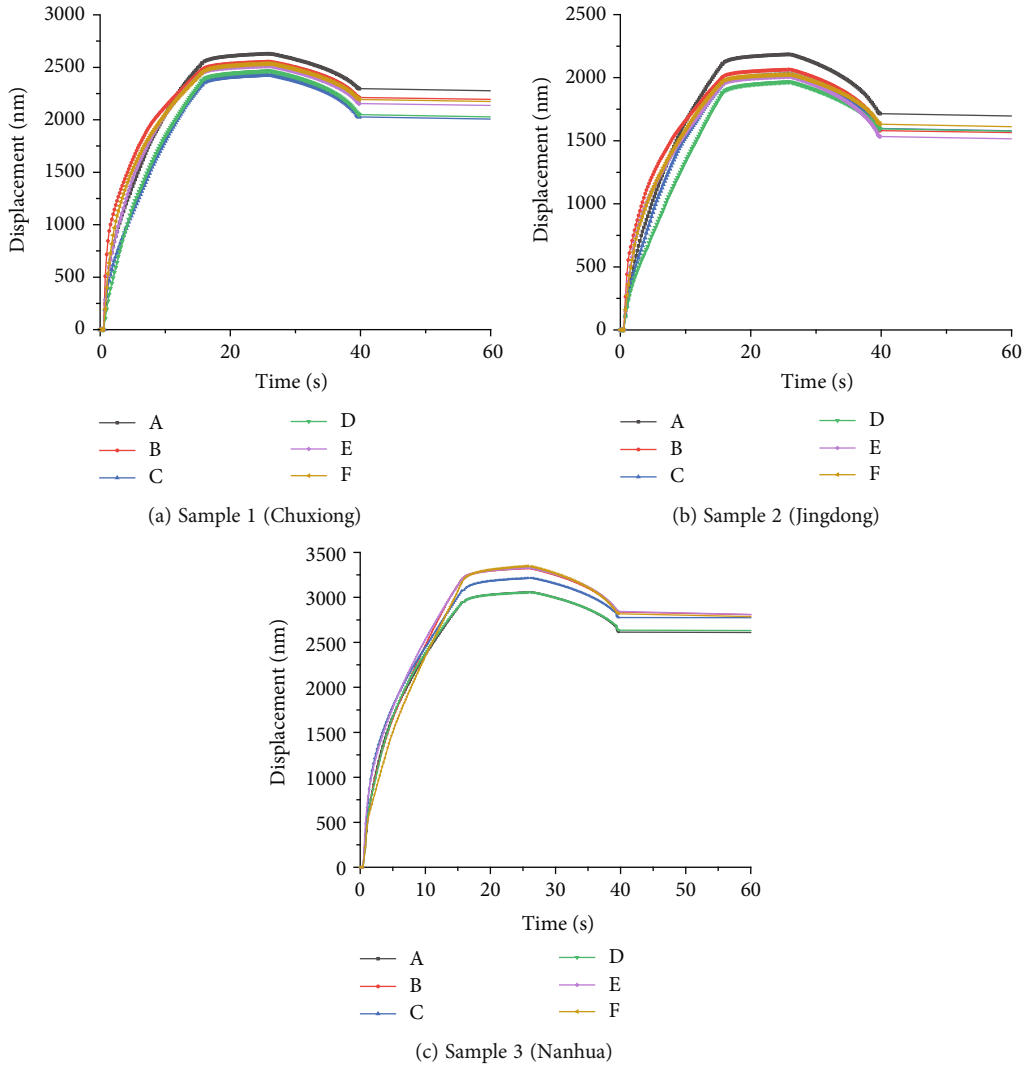

Figure 12: Nanoindentation displacement-time curves of Yunnan red-bed mudstone samples in three regions.

relatively smooth and flat area. This area should be able to lay a certain number of points evenly to avoid the dense effect.

2.4.6. Loading Stage. The loading-holding-unloading mode was adopted in nanoindentation tests. The maximum load is 100 mN. The loading time and the unloading time are both 15 s. The holding time is 10 s. The load-time curve is shown in Figure 7. After setting the parameters, the program was started to do the dots by a nanoindenter. The specific schematic diagram is shown in Figure 8.

2.4.7. Processing Data. The experimental data was processed by using *Nanosuite* software.

3. Comparative Analysis of Nanomechanical Properties of Yunnan Red-Bed Mudstone

3.1. Result Analysis of Thin Section Examination Test of Red-Bed Mudstone in Different Regions. The thin-section mesostructure of Yunnan red-bed mudstone in three regions is shown in Figure 9. It can be found that the clastic rock content of sample 1 (Chuxiong) is 52%, calcite content is 27%, chlorite content is 6%, and clastic crystal quartz content is 15%; quartz crystal content of sample 2 (Jingdong) is 36%, calcite crystal content is 14%, chlorite content is 12%, limonite content is 25%, and chalcedony content is 13%; calcite content of sample 3 (Nanhua) is 34%, clastic rock content is 41%, chlorite content is 6%, clastic crystal calcite content is 6%, and clastic crystal quartz content is 13%.

3.2. Residual Indentation Morphology Analysis of Red-Bed Mudstone in Different Regions. Comparative analysis of residual indentation morphology of Yunnan red-bed mudstone in the three regions is shown in Figure 10. Under the same loading and holding time conditions, sample 3 (Nanhua) has the deepest residual indentation, and SEM tests show that the damage to indentation is obvious. Sample 2 (Jingdong) has the shallowest residual indentation. The indentation morphology is complete and the size is small by SEM tests. The residual indentation depth of sample 1 (Chuxiong) is between sample 2 and sample 3.

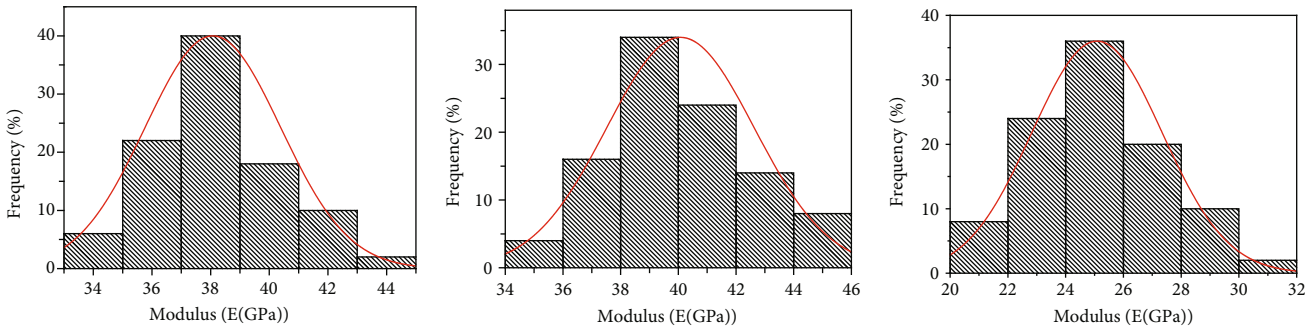

(a) Sample 1 (Chuxiong) (b) Sample 2 (Jingdong) (c) Sample 3 (Nanhua)

Figure 13: Normal distribution diagrams of elastic modulus of Yunnan red-bed mudstone in three regions.

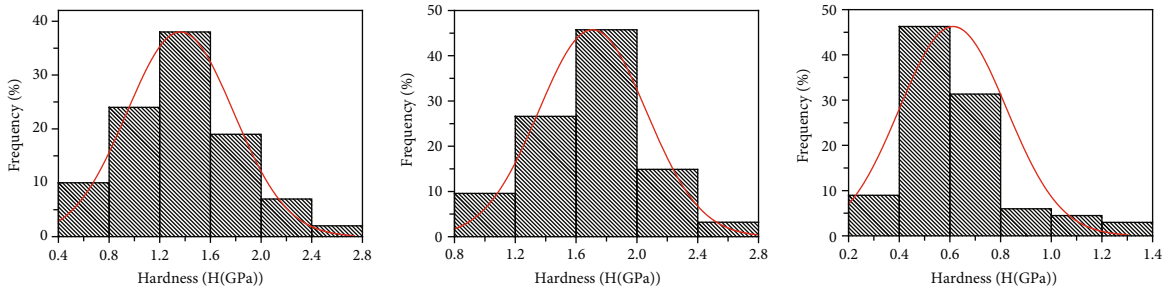

(a) Sample 1 (Chuxiong) (b) Sample 2 (Jingdong) (c) Sample 3 (Nanhua)

Figure 14: Normal distribution diagrams of hardness of Yunnan red-bed mudstone in three regions.

3.3. Analysis of nanomechanical indexes of Red-Bed Mudstone in Different Regions. The nanoindentation load-displacement curves of Yunnan red-bed mudstone samples in three regions are shown in Figure 11. It can be seen that the indentation displacement of sample 3 (Nanhua) is the largest and the indentation displacement of sample 2 (Jingdong) is the smallest under the same loading and holding conditions. The nanoindentation displacement-time curves of Yunnan red-bed mudstone samples in three regions are shown in Figure 12. It can be seen that the residual indentation depth of sample 1 (Chuxiong) is 2073.00 nm, the residual indentation depth of sample 2 (Jingdong) is 1540.45 nm, and the residual indentation depth of sample 3 (Nanhua) is 2508.66 nm. It shows that sample 2 (Jingdong) has the best mechanical properties, then sample 1 (Chuxiong), and sample 3 (Nanhua) has the worst.

The statistical analysis diagrams of elastic modulus and hardness of Yunnan red-bed mudstone in three regions are shown in Figures 13 and 14, respectively. It can be seen that elastic modulus and hardness distribution of Yunnan red-bed mudstone in the three regions conform to the normal distribution. Among them, sample 2 (Jingdong) has the smallest elastic modulus distribution span, while sample 1 (Chuxiong) and sample 3 (Nanhua) have larger distribution spans. It is found that the elastic modulus of sample 1 (Chuxiong) is 38.0 ± 2.29 GPa and hardness is 1.36 ± 0.42 GPa, elastic modulus of sample 2 (Jingdong) is 40.1 ± 2.03 GPa and hardness is 1.71 ± 0.35 GPa, and elastic modulus of sample 3 (Nanhua) is 25.1 ± 2.53 GPa and hardness is 0.61 ± 0.21 GPa. Due to the high content of quartz crystal in sample 2 (Jingdong), its mechanical properties are the best.

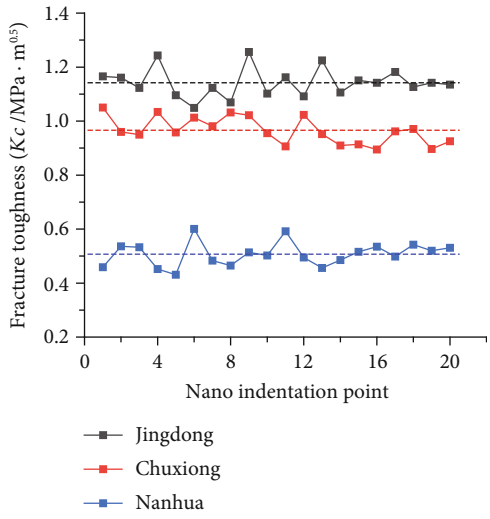

Figure 15: Fracture toughness distribution of Yunnan red-bed mudstone in three regions.

Through nanoindentation load-displacement curves, fracture toughness of sample 1 (Chuxiong), sample 2

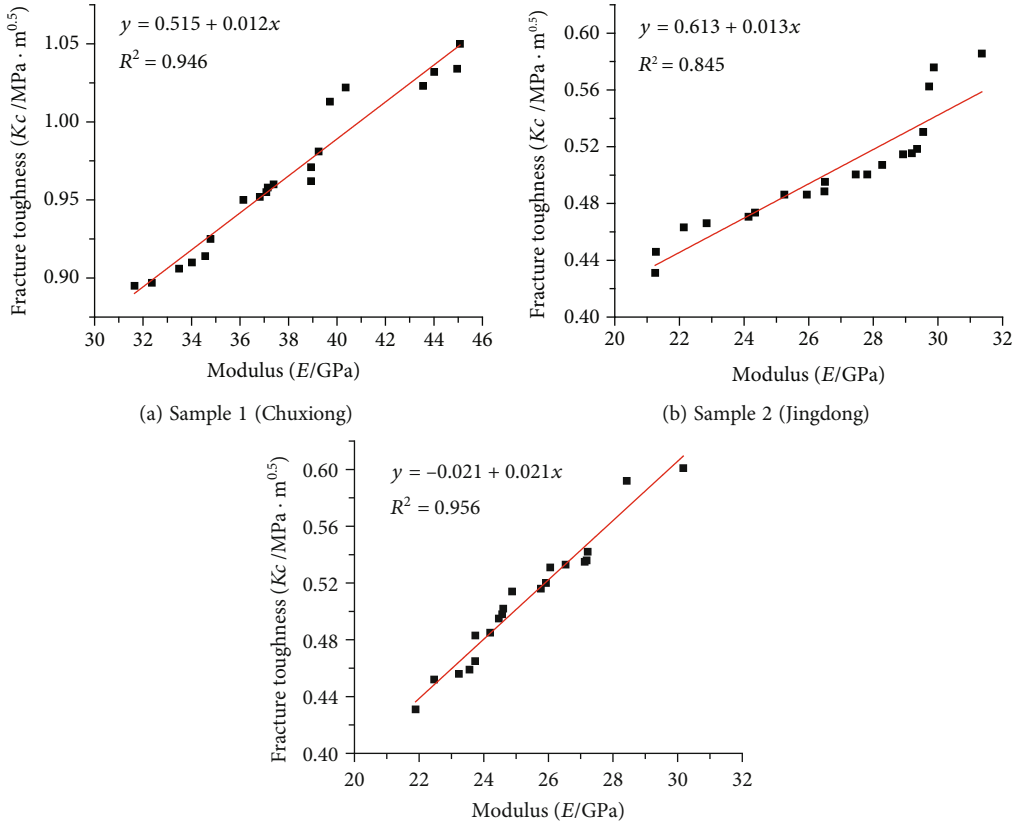

(a) Sample 1 (Chuxiong)

(b) Sample 2 (Jingdong)

(c) Sample 3 (Nanhua)

Figure 16: Fitting curve of mudstone fracture toughness and elastic modulus.

(Jingdong), and sample 3 (Nanhua) is calculated based on the energy analysis method, as shown in Figure 15. The average fracture toughness of sample 1 (Chuxiong), sample 2 (Jingdong), and sample 3 (Nanhua) is 0.966 ± 0.048 MPa·m$^{0.5}$, 1.142 ± 0.053 MPa·m$^{0.5}$, and 0.507 ± 0.043 MPa·m$^{0.5}$, respectively. It can be seen that the fracture toughness of minerals with large elastic modulus is relatively large.

4. Discussion

The relationship between fracture toughness and elastic modulus of red-bed mudstone in three regions is shown in Figure 16, respectively. It can be seen that the relationship between fracture toughness and elastic modulus is linear. This is because the increase in elastic modulus can increase ultimate fracture strength, thereby improving fracture resistance [20].

Compared with macromechanical indexes, elastic modulus, hardness, and fracture toughness of red-bed mudstone are larger. This is because the size of the indentation head is very small in the nanoindentation test, and the mineral crystals around the indentation act on the indentation head, which is equivalent to the confining pressure effect on the sample in the macrotest. The corresponding mechanical properties under confining pressure will be further studied in subsequent tests.

5. Conclusion

With the planning and construction of the Yunnan expressway and railway networks, more and more red-bed mudstone engineering disasters have emerged. Understanding and mastering the macro- and micromechanical properties of red-bed mudstone are of great significance to engineering construction. Taking Yunnan red-bed mudstones in three regions as the research objects, micromechanical parameters of red-bed mudstones were obtained by nanoindentation tests. A comparative analysis of micromechanical properties of red-bed mudstones in different areas in Yunnan was carried out. The main conclusions are as follows:

(1) The average elastic modulus of sample 1 (Chuxiong) is 38.0 ± 2.29 GPa. The average hardness is 1.36 ± 0.42 GPa, and the fracture toughness is 0.966 ± 0.048 MPa·m$^{0.5}$. The average elastic modulus of sample 2 (Jingdong) is 40.1 ± 2.03 GPa. The average hardness is 1.71 ± 0.35 GPa, and the fracture toughness is 1.142 ± 0.053 MPa·m$^{0.5}$. However, the average elastic modulus of sample 3 (Nanhua) is 25.1 ± 2.53 GPa. The average hardness is 0.61 ± 0.21 GPa, and the fracture toughness is 0.507 ± 0.043 MPa·m$^{0.5}$

(2) The residual indentation depth of sample 1 (Chuxiong) is about 2000 nm, the residual indentation

depth of sample 2 (Jingdong) is about 1500 nm, and the residual indentation depth of sample 3 (Nanhua) is about 2500 nm. It shows that sample 2 (Jingdong) has the best mechanical properties, then sample 1 (Chuxiong), and sample 3 (Nanhua) has the worst

(3) It can be seen from nanomechanical indexes of Yunnan red-bed mudstones in the three regions that three samples are from the center of Yunnan and belong to red-bed mudstones, but the micromechanical properties of them are quite different. Therefore, it can be inferred that there are great differences in macroscopic mechanical properties and reveals the regional differences in the distribution of red-bed mudstone

Data Availability

All data included in this study are available upon request by contact with the corresponding author.

Conflicts of Interest

The authors declare no conflict of interest.

Acknowledgments

The study was funded by the Science and Technology Innovation Program of the Department of Transportation in Yunnan Province of China (No.: 2019301), National Natural Science Foundation of China (No.: 52009107), China Postdoctoral Science Foundation (No.: 2019M663943XB), Natural Science Basic Research Plan in Shaanxi Province of China (No.: 2020JQ-627), Opening Research Fund of National Engineering Laboratory for Surface Transportation Weather Impacts Prevention (NEL-2020-02), and National Science and Technology Major Project of China (No.: 2018YFC1504906).

References

[1] G. N. Kalei, "Some results of microhardness test using the depth of impression," *Mashinovedenie*, vol. 4, no. 3, pp. 105–107, 1968.

[2] W. C. Oliver and G. M. Pharr, "An improved technique for determining hardness and elastic modulus using load and displacement sensing indentation experiments," *Journal of Materials Research*, vol. 7, no. 6, pp. 1564–1583, 1992.

[3] X. Shi, Z. He, S. Long, Y. Peng, D. Li, and S. Jiang, "Loading rate effect on the mechanical behavior of brittle Longmaxi shale in nanoindentation," *International Journal of Hydrogen Energy*, vol. 44, no. 13, pp. 6481–6490, 2019.

[4] X. Shi, S. Jiang, L. Yang, M. Tang, and D. Xiao, "Modeling the viscoelasticity of shale by nanoindentation creep tests," *International Journal of Rock Mechanics and Mining Sciences*, vol. 127, 2020.

[5] K. Liu, M. Ostadhassn, and B. Bubach, "Applications of nanoindentation methods to estimate nanoscale mechanical properties of shale reservoir rocks," *Journal of Natural Gas Science and Engineering*, vol. 35, pp. 1310–1319, 2016.

[6] C. Sun, G. Li, M. E. Gomah, J. Xu, and H. Rong, "Meso-scale mechanical properties of mudstone investigated by nanoindentation," *Engineering Fracture Mechanics*, vol. 238, article 107245, 2021.

[7] C. Sun, G. Li, M. E. Gomah, J. Xu, and H. Rong, "Experimental investigation on the mechanical properties of crushed coal samples based on the nanoindentation technique," *Journal of China Coal Society*, vol. 45, Supp. 2, pp. 682–691, 2020.

[8] F. Zhang, H. Guo, J. Zhao, D. Hu, Q. Sheng, and J. Shao, "Experimental study of micro-mechanical properties of granite," *Chinese Journal of Rock Mechanics and Engineering*, vol. 36, no. Supp.2, pp. 3864–3872, 2017.

[9] G. L. Manjunath and B. Jha, "Nanoscale fracture mechanics of Gondwana coal," *International Journal of Coal Geology*, vol. 204, pp. 102–112, 2019.

[10] Y. Zhang, M. Lebedev, A. Al-Yaseri et al., "Nanoscale rock mechanical property changes in heterogeneous coal after water adsorption," *Fuel*, vol. 218, pp. 23–32, 2018.

[11] P. Chen, Q. Han, T. Ma, and D. Lin, "The mechanical properties of shale based on micro-indentation test," *Petroleum Exploration and Development*, vol. 42, no. 5, pp. 723–732, 2015.

[12] X. Shi, S. Jiang, S. Lu et al., "Investigation of mechanical properties of bedded shale by nanoindentation tests: a case study on Lower Silurian Longmaxi Formation of Youyang area in southeast Chongqing, China," *Petroleum Exploration and Development*, vol. 46, no. 1, pp. 155–164, 2019.

[13] Z. Dou, Z. Zhao, T. Gao, J. Li, and Q. Yang, "Evolution law of water-rock interaction on the shear behabior of granite fractures," *Journal of Tsinghua University (Science and Technology)*, vol. 61, no. 8, pp. 792–798, 2021.

[14] S. Liu, Z. Wang, L. Zhang, and L. Ma, "Micromechanics properties analysis of shale on nano-indentation," *Journal of Experimental Mechanics*, vol. 33, no. 6, pp. 957–968, 2018.

[15] S. P. Graham, M. Rouainia, A. C. Aplin, P. Cubillas, T. D. Fender, and P. J. Armitage, "Geomechanical characterisation of organic-rich calcareous shale using AFM and nanoindentation," *Rock Mechanics and Rock Engineering*, vol. 54, pp. 303–320, 2021.

[16] J. L. Zhao, D. X. Zhang, T. H. Wu et al., "Multiscale approach for mechanical characterization of organic-rich shale and its application," *International Journal of Geomechanics*, vol. 19, no. 1, pp. 04018180-1–04018180-16, 2019.

[17] W. C. Oliver and G. M. Pharr, "Measurement of hardness and elastic modulus by instrumented indentation: advances in understanding and refinements to methodology," *Journal of Materials Research.*, vol. 19, no. 1, pp. 3–20, 2004.

[18] Y. T. Cheng, Z. Y. Li, and C. M. Cheng, "Scaling relationships for indentation measurements," *Philosophical Magazine A*, vol. 82, no. 10, pp. 1821–1829, 2002.

[19] G. D. Quinn and R. C. Bradt, "On the Vickers indentation fracture toughness test," *Journal of the American Ceramic Society.*, vol. 90, no. 3, pp. 673–680, 2007.

[20] C. C. Yuan and X. K. Xi, "On the correlation of Young's modulus and the fracture strength of metallic glasses," *Journal of Applied Physics*, vol. 109, no. 3, pp. 033515-1–033515-5, 2011.